Journal of Organometallic Chemistry, 417 (1991) 327–338
Elsevier Sequoia S.A., Lausanne
JOM 21999

Mercury(II) and thallium(III) organometallic derivatives of 2-Mercaptobenzoxazole

M.V. Castaño *, H. Calvo, A. Sánchez, J.S. Casas, J. Sordo

Departamento de Química Inorgánica, Universidade de Santiago de Compostela, 15706 Santiago de Compostela (Galicia) (Spain)

Y.P. Mascarenhas *

Instituto de Física e Química de Sao Carlos, Universidade de Sao Paulo, 13560 Sao Carlos SP (Brazil)

and C. de O.P. Santos

Departamento de Ciencias Ambientais, FCT, UNESP, 19100, Presidente Prudente, SP (Brazil)

(Received March 20th, 1991)

Abstract

Some derivatives of 2-mercaptobenzoxazole (HL) of the type MR_nL [M = Hg or Tl, R = Me or Ph and $n = 1$ (Hg) or 2 (Tl)] have been prepared. The structure of HgMeL has been determined by an X-ray diffraction study; in the crystal there are two independent planar molecules in each asymmetric unit, with the ligand in its thiolic form and an almost linear C–Hg–S linkage. Weak intramolecular and intermolecular secondary interactions complement the mercury–sulphur bond. The spectroscopic (IR, Raman, mass, ^{13}C-NMR), conductimetric, and dipolar properties of this and the other compounds are discussed.

Introduction

Some years ago Carty [1] pointed out that the low residual Lewis acidity in MeHgSR complexes is of major significance in the context of methylmercury mobility in biological systems. This residual acidity leads to formation of "secondary bonds" [2]. Some of these interactions are associated with short bond distances [3,4], and probably contribute significantly to the final stability of the compounds.

In our studies of such "secondary bonds" in organomercury derivatives containing heterocyclic ligands capable of thione/thiol tautomerism [5–7], we found evidence in the solid state of weak bonding interactions between mercury and nitrogen atoms or between mercury and the π charge of a C–N bond which lead to a "pseudo chelating" coordinative mode of the ligand. In (2-mercaptobenzothiazolato)methylmercury(II) [5] some additional close contacts between the metal and the intraanular sulphur atom have also been detected, although these distances,

0022-328X/91/$03.50 © 1991 – Elsevier Sequoia S.A. All rights reserved

which approach the sum of the Van der Waals radii, could be imposed by the packing.

We have now succeeded in preparing some compounds of 2-mercaptobenzoxazole (HL) and in determining the structure of HgMeL. In this ligand, L, the annular sulphur of the 2-mercaptobenzothiazole is replaced by an oxygen atom. The structural data for HgMeL together with some relevant spectroscopic (mass, IR, Raman and ^{13}C NMR) data for this and related compounds (HgPhL, $TlMe_2L$, $TlPh_2L$) are presented in this paper. Diorganothallium compounds have been included for purposes of comparison.

Experimental

The reagents HL, HgMeCl, and HgPhAc were obtained commercially and used without further purification. $TlMe_2I$ and $TlPh_2Br$ were prepared as described elsewhere [8].

Synthesis of the compounds

To a stirred methanolic solution of HL was slowly added an aqueous solution of an equimolar amount of methylmercury(II) hydroxide [obtained by stirring HgMeCl for several hours with an aqueous suspension of freshly prepared silver oxide]. The white solid formed was filtered off and dried under reduced pressure. The phenylmercury(II) derivative was a similarly obtained by use of an ethanolic solution of phenylmercury(II) acetate, and $TlMe_2L$ was prepared as described previously [9]. The diphenylthallium(III) compound was obtained by slow addition of a solution of an equimolar amount of $TlPh_2Br$ in water made basic with KOH to an aqueous solution of the ligand. The mixture was refluxed for 10 h and the solid formed was filtered off, refluxed with methanol until all the residual $TlPh_2Br$ had been extracted, and then again filtered off and vacuum dried.

Analytical data (Carlo Erba Mod 1108 apparatus) and some physical properties of the prepared compounds are given in Table 1.

Determination of the crystal structure

One of the syntheses of HgMeL gave monocrystals suitable for X-ray diffraction measurements. A needle-shaped single crystal with the y axis along the needle direction and dimensions of 0.5 mm length and 0.13 mm diameter was used for crystal data and intensity measurements.

Crystal data. C_8H_7ONSHg, $M = 365.74$, monoclinic, space group $P2_1$, $a = 10.601(1)$, $b = 8.164(3)$, $c = 10.876(2)$ Å, $\beta = 103.87(1)°$, $V = 913.8(6)$ Å^3, $Z = 4$ with two independent molecules per asymmetric unit specified as I and I′, $D_x = 2.51$ g/cm^3, $\mu = 163.86$ cm^{-1}, λ(Mo-K_α) = 0.71073 Å, $F(000) = 664$.

Data collection and processing. Data were obtained at ca. 293 K on a CAD-4 Enraf–Nonius diffractometer. Intensity data were collected in the 2θ range from 1 to 25°, hkl range: $-12 \leqslant h \leqslant +12$, $0 \leqslant k \leqslant 9$, $0 \leqslant l \leqslant +12$ using ω–2θ scan width given by $0.8 + 0.35\text{tg}\theta$. A total of 1725 reflections were measured, 1247 of these with $I > 3\sigma(I)$. Two standard reflections (040) and (602) were monitored every 500 reflections and the intensity variation shown to be < 1.7%. Intensities were corrected for L_p and an empirical absorption correction [10] was applied.

Table 1

Analyses and some physical data for the new compounds

	%C	%H	%N	%S	M.p. (°C)	Λ (ohm^{-1} cm^2 mol^{-1}) [d]
HgMeL	26.39	1.93	3.82	9.36	106(D) [b]	2.1
	(26.26) [a]	(1.91)	(3.83)	(8.75)		
HgPhL	36.54	2.28	3.35	7.53	135(D) [b]	2.6
	(36.46)	(2.10)	(3.27)	(7.48)		
$TlMe_2L$	28.27	2.75	3.57	8.43	139	1.7
	(28.10)	(2.62)	(3.64)	(8.32)		
$TlPh_2L$	43.53	2.81	2.58	6.98	247	[c]
	(44.85)	(2.77)	(2.75)	(6.29)		

[a] Theoretical values in brackets. [b] D = Decomposition. [c] Non soluble. [d] Molar conductivity for 10^{-3} *M* solutions in acetonitrile.

Structure analysis and refinement. The structure was determined by Patterson and difference Fourier methods. A block-diagonal least-squares refinement was performed anisotropically for Hg, S, C(1), N and O, and isotropically for the phenyl

Table 2

Final fractional atomic coordinates and equivalent temperature factors for HgMeL (esd's in parentheses)

Atom	*x*	*y*	*z*	B_{iso}
C(8)	0.004(4)	−0.411(7)	0.238(4)	5.2(9)
Hg	0.1221(1)	−0.3118(3)	0.1222(1)	3.78(4)
S	0.261(1)	−0.180(2)	0.0073(9)	4.0(3)
C(1)	0.383(3)	−0.095(6)	0.138(3)	4.(1)
N	0.366(3)	−0.123(3)	0.256(3)	3.9(8)
O	0.478(3)	−0.011(4)	0.120(3)	3.4(9)
C(2)	0.477(3)	−0.041(6)	0.334(3)	3.6(6)
C(3)	0.546(3)	0.020(4)	0.243(3)	2.9(6)
C(4)	0.655(4)	0.111(6)	0.294(4)	4.1(7)
C(5)	0.696(4)	0.132(5)	0.427(4)	3.9(7)
C(6)	0.621(4)	0.058(6)	0.505(4)	4.8(9)
C(7)	0.509(4)	−0.031(7)	0.458(4)	5.0(8)
C(8′)	0.606(4)	0.558(6)	0.226(4)	4.3(8)
Hg′	0.4405(1)	0.4564(3)	0.1117(1)	3.75(4)
S(1′)	0.246(1)	0.330(2)	−0.0031(9)	4.3(3)
C(1′)	0.185(4)	0.251(5)	0.111(4)	4.(1)
N′	0.257(3)	0.262(4)	0.236(3)	4.4(9)
O′	0.076(3)	0.171(5)	0.110(3)	4.(1)
C(2′)	0.180(3)	0.176(5)	0.309(3)	3.6(6)
C(3′)	0.068(4)	0.117(6)	0.229(4)	4.3(8)
C(4′)	−0.015(5)	0.041(7)	0.274(5)	6.(1)
C(5′)	0.010(5)	0.005(6)	0.406(4)	5.1(9)
C(6′)	0.127(4)	0.072(6)	0.488(4)	4.2(7)
C(7′)	0.219(3)	0.160(4)	0.443(3)	3.0(6)
H(81)	0.0583	−0.4875	0.2173	5.2
H(82)	−0.0861	−0.3413	0.1674	5.2
H(83)	−0.0291	−0.4136	0.3249	5.2
H(81′)	0.5954	0.6814	0.1493	4.3
H(82′)	0.6972	0.3263	0.2321	4.3
H(83′)	0.6114	0.6560	0.3133	4.3

Table 3

Interatomic distances (Å) for HgMeL

	I	I′
Intramolecular distances		
C(8)–Hg	2.06(5)	2.05(4)
Hg–S(1)	2.40(1)	2.40(1)
Hg–C(1)	3.20(4)	3.24(4)
Hg–N	3.08(3)	3.05(3)
S(1)–C(1)	1.78(4)	1.72(4)
C(1)–N	1.31(4)	1.43(5)
C(1)–O	1.33(5)	1.27(5)
N–C(2)	1.38(5)	1.41(5)
O–C(3)	1.37(4)	1.39(5)
C(2)–C(3)	1.41(5)	1.35(6)
C(2)–C(7)	1.40(5)	1.47(5)
C(3)–C(4)	1.38(5)	1.34(7)
C(4)–C(5)	1.43(6)	1.43(7)
C(5)–C(6)	1.35(6)	1.47(6)
C(6)–C(7)	1.47(7)	1.32(6)
Intermolecular distances		
Hg^{a}–S(1)′	3.61(1)	
Hg^{b}–O′	2.86(3)	
S(1)–Hg′^{c}	3.56(1)	
O–Hg′^{d}	2.89(3)	

Symmetry operations: ^{a} $x,1+y,z$; ^{b} $-x,1/2+y,-z$; ^{c} $x,y-1,z$; ^{d} $1-x,y-1/2,-z$.

and methyl carbon atoms; in alternate cycles the coordinates of one of the molecules in the asymmetric unit were fixed. Owing to the very similar electron densities on the N and O atoms, these atoms could not be distinguished from one another. Hydrogen atoms were placed in calculated positions and their temperature parameters were fixed at twice the value for the isotropic thermal parameters of the atom to which they were bound. Final R and R_w $\{w=[\sigma(F)+0.003F]^{-2}\}$ were 0.077 and 0.076; when the coordinates were inverted there was no significant change in these values. All calculations were performed using the SHELX76 program package [11]. Tables of thermal parameters and final structure factors are available from the authors. Final positional and equivalent isotropic temperature parameters with esd's in parentheses are listed in Table 2. Interatomic distances and angles are listed in Tables 3 and 4. Figure 1 shows the molecular structure and the atom labelling, and Fig. 2 a stereoview of the crystal structure .

Other physicochemical measurements

Dipole moments (For HgRL compounds) were determined in benzene at 25°C as reported previously [12]. Conductivities were measured in acetonitrile with a WTW LF3 conductimeter. FAB mass spectra (8 keV, Xe atoms; 3-nitrobenzyl alcohol, glycerol, or thioglycerol matrix) were obtained with a Kratos MS50TC apparatus. ^{13}C NMR spectra were recorded for DMSO-d_6 solution on a Bruker WM250 spectrometer at 62.83 MHz, and the ^{13}C CP/MAS spectrum of HgMeL on a Bruker MSL-400 apparatus at 100.63 MHz using zirconia rotors spinning at 4.0 KHz [spectral parameters were: spectral width 100 kHz, adquisition time 20 ms,

Table 4

Bond angles (°) for HgMeL

	I	I′
C(8)–Hg–S(1)	173.(1)	175.(1)
Hg–S(1)–C(1)	99.(1)	103.(1)
S(1)–C(1)–N	121.(1)	115.(1)
S(1)–C(1)–O	122.(1)	130.(1)
C(1)–N–C(2)	103.(1)	98.(1)
C(1)–O–C(3)	104.(1)	109.(1)
N–C(2)–C(3)	108.(1)	99.(1)
N–C(2)–C(7)	124.(1)	97.(1)
C(3)–C(2)–C(7)	128.(1)	123.(1)
O–C(3)–C(2)	107.(1)	104.(1)
O–C(3)–C(4)	133.(1)	134.(1)
C(2)–C(3)–C(4)	119.(1)	122.(1)
C(3)–C(4)–C(5)	116.(1)	119.(1)
C(4)–C(5)–C(6)	125.(1)	118.(1)
C(5)–C(6)–C(7)	121.(1)	123.(1)
C(2)–C(7)–C(6)	111.(1)	115.(1)

recycle delay 6 s, 600 transients. A TOSS pulse sequence (13) was used to eliminate spinning side bands]. IR spectra were recorded with Nujol mulls or KBr pellets on a Perkin–Elmer 180 spectrometer, and Raman spectra on a Jarrel-Ash 500 apparatus (Ar^+ laser, 5145 Å). Fluorescence prevented recording of the Raman spectrum of the HgPhL compound.

Results and discussion

X-Ray structure of HgMeL

In the crystal, both independent molecules, I and I′, are planar with an average atomic deviation from the plane of the molecule of ±0.02 and ±0.04 Å, respectively. In spite of the high esd values and the rather large differences between some angles and distances of molecules I and I′, there are clear differences between the bond parameters for the ligand and those for the free ligand [14]. The C(1)–S bond distance is increased as a result of the sulphur–mercury bond formation, in accord with a thione to thiol transformation. Deprotonation of the N–H group would be expected to lead to a decrease in the C(1)–N–C(2) angle [15], but the C(1)–O–C(3) angle should be less affected by the thione–thiol change. The assignment of the two heteroatoms in the pentagonal ring of the ligand (Fig. 1) was made in the light of these facts. The atom involved in the angle that is almost unchanged by complexation (molecule I′) or that changes the least, was identified as the oxygen atom.

The mercury atom has an almost linear stereochemistry, with normal Hg–S and Hg–C(8) distances and S–Hg–C(8) angle. As in other complexes of heterocyclic ligands with the thioimide group, the planarity of the molecules and the location of the metal close to the C(1)–N part of the pentagonal ring suggest the existence of some additional weak intramolecular interaction. The Hg···N and Hg···C(1) distances, which are smaller than the sum of the Van der Waals radii for the atoms concerned [16], confirm the presence of a secondary interaction in this part of the

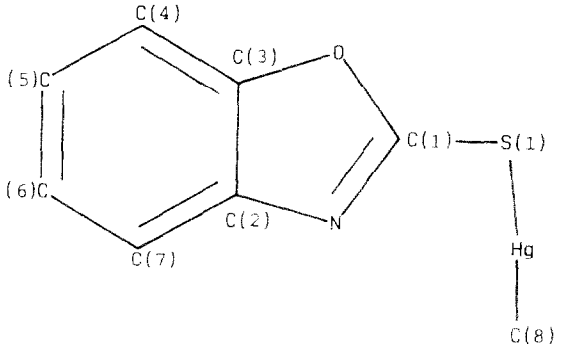

Fig. 1. Molecular structure of HgMeL with the atom numbering scheme.

molecule similar to that observed in (2-mercaptobenzothiazolato)methylmercury(II) [5]. However, unlike the latter compound, with (2-mercaptobenzoxazolato)methylmercury(II) there is also an intermolecular interaction through the oxygen atom (Fig. 2), with an Hg · · · O distance close to that observed in methylmercury(II)-2-*S*-methylthiouracylate [17]. Because of this interaction the crystal can be regarded as made up of infinite chains aligned along the x axis.

Mass spectra

The mercury compounds show identical ionization patterns, the dominant peaks coming from the ions $[M + H]^+$ and $[M + HgR]^+$ (Table 5). Figure 3 shows the measured and calculated isotope distribution for $[M + HgMe]^+$. Plausible structures for these ions are:

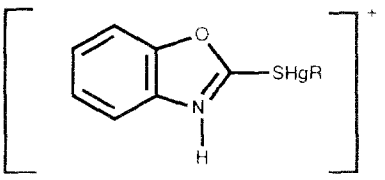

(I)

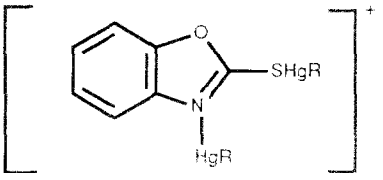

(II)

The high intensities of the pseudomolecular ions $[M + H]^+$ (the base peaks in the spectra of the HgRL compounds) indicate that FAB-MS is a very valuable tool for the study of this type of complexes. As expected, thermal decomposition fragments usually found for PhHg derivatives when EI and CI techniques are applied ([18] and

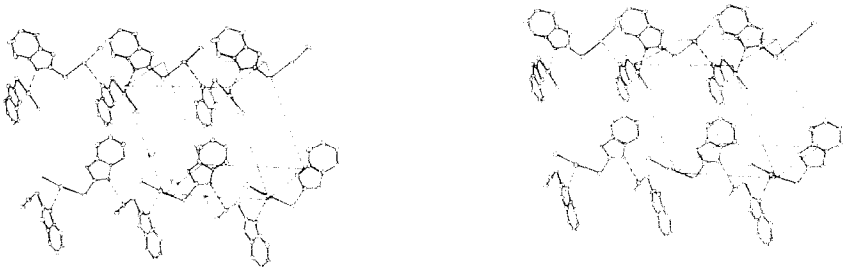

Fig. 2. Stereoview of the HgMeL structure, showing weak intermolecular interactions.

Table 5

The most relevant FAB-MS data for MR_nL complexes

ION	Ion abundance (m/z) [a]			
	HgMeL	HgPhL	$TlMe_2L$	$TlPh_2L$
$[2M+H]$	3.3(733)	2.6(857)	–	–
$[M+MR_n]$ [b]	40.7(582)	28.8(706)	38.9(620)	–
$[M+MR_n-2R]$	–	–	11.3(590)	–
$[M+MR_n-4R]$	–	–	4.8(560)	–
$[M+H]$	100(368)	100(430)	–	–
$[MR_n]$	9.6(217)	18.3(279)	100(235)	8.9(359) [c]
[M]	–	–	66.4(205)	6.4(205) [c]

[a] Masses of monometalled species are based on the major isotopes ^{202}Hg and ^{205}Tl. The values for dimetallated species refires to the most intense peak of the isotopic pattern. [b] M = Hg or Tl. [c] Base peak $[TlPh_2MNBA]$.

references therein), were not observed. A small concentration of the dinuclear ions $[2M+H]^+$ was also detected, together with the very stable $[HgR]^+$ ions normally present in the EI or CI spectra [18].

The mass spectra of the thallium derivatives were different, exchange reactions with the matrix being important. Thus the spectrum of $TlPh_2L$ in 3-nitrobenzyl

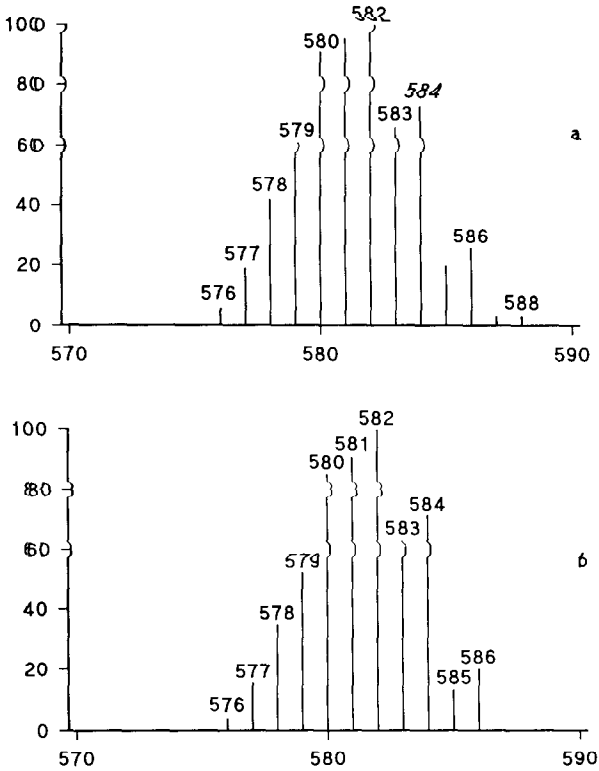

Fig. 3. Measured (a) and calculated (b) isotopic distribution for the $[M+HgMe]$ ion.

alcohol (MNBA) showed the [$TlPh_2$MNBA] and [$TlPh_2$] ions as the only metallated species. $TlMe_2L$ was more stable towards ligand/matrix exchange, and the peak for the ion of type II was clearly observed, as were the peaks for the ions $[M + TlMe_2 - 2Me]^+$ and $[M + TlMe_2 - 4Me]^+$. Nevertheless, the [$TlMe_2$MNBA] ion signal was again very intense (see Table 5).

The displacement of the ligand by the matrix was further examined in the case of the thallium compounds using glycerol and thioglycerol (TG) matrices. With glycerol exchange still occurs for $TlMe_2L$, but ions type I and II can be observed ($TlPh_2L$ was not soluble in glycerol). Although, in TG the peaks for these ions were also present, there was more ligand/matrix exchange and a new ion ([$2TlMe_2$ + TG − H]) was detected (10%). The $TlPh_2L$ spectrum was also dominated by the ion $[2TlPh_2 - TG - H]^+$ and other $TlPh_2$/TG derived ions: $[M + TlPh_2 - 4Ph]^+$ was the only in arising from the initial complex alone.

IR and Raman spectra

The significant bands of the ligand [19–21] and its complexes are shown in Table 6. The bands assigned in the free ligand to the ν(N–H) and δ(N–H) modes disappear in the complexes due to the deprotonation of the ligand. In the 1600–1400 cm^{-1} range the changes in the ligand spectrum under complexation follow the pattern previously described for 2-mercaptobenzothiazole in complexes in what this ligand is S-bonded and its C=N group also participates in metal coordination [5,9,19,22]. The behaviour of the other major bands in the spectra of the complexes is compatible with this type of coordination, although the band at 745 cm^{-1}, previously assigned as the thioamide IV band (that is, essentially to the ν(C=S) mode [19]) is not shifted to lower wavenumbers as would be expected for S-coordination. This shift is nevertheless observed for the 675 cm^{-1} band, which is assigned as the thioamide IV band in Table 6.

The weak Hg · · · O intermolecular interaction detected by the X-ray study in the case of HgMeL does not load to any shift in the ν(C–O–C) band, so the possible presence of this secondary bond in the other complexes cannot be assessed this way. The ν(C–Tl–C) and ν(Hg–C) vibrations lie close to the position observed previously for complexes with related S-bonded ligands [5,9] and, as in those systems, the bands assigned to ν(Hg–S) are possibly not pure.

Conductivity

All the compounds are soluble in DMSO and, except for $TlPh_2L$, in common organic solvents, but not in water. Conductivity measurements in acetonitrile (Table 1) show all the complexes to be non-electrolytes [23].

Dipole moments

Only the organomercuric derivatives were sufficiently soluble in benzene for dipole moment measurements. The observed dipole moments for these compounds were 1.92 D (HgMeL) and 1.99 D (HgPhL). Although the asymmetry of the ligand ring makes quantitative analysis of these values difficult, approximate conclusions can be reacted on the basis of the following assumptions: (i) The moments of the (C–O=C) and (C–N=C) groups in the oxazole ring are the same as those of tetrahydrofuran (1.75 D) and pyridine (2.2 D) [24]; (ii) These group moments are oriented along the bisector of the corresponding angles, where these angles are as in

Table 6

Major bands in the IR and Raman spectra of HL and its complexes

Ligand	HgMeL		HgPhL	$TlMe_2L$		$TlPh_2L$		Assignment
IR	IR	R	IR	IR	R	IR	R	
3300–3200m,b	–	–	–	–	–	–	–	ν(NH)
1510s	1475m	1485m	1480m	1465m		1480m	1480w	thioamide I
1450s	1450s	1460s	1450s	1450m	1450s	1450m	1450s	ring stretching
			1430m	1430s		1430s		
1245m	1240s	1230w	1240s	1245s	1230w	1240s	1235m	thioamide II
1095s	1090m	–	1090m	1080m	–	1090m	–	ν_{as}(COC)
1010m	1005m	1015m	1015m	1010m	1015m	1020m	1015s	thioamide III
815m	810m	820m	810m	810m	820m	810m	825m	ν_s(COC)
675m	–	645m	–	–	660m	–	680w	thioamide IV
							670w	
650s,b	–	–	–	–	–	–	–	δ(NH)
				550m	–			ν_{as}(C–Tl–C)
				540m				
				–	485vs			ν_s(C–Tl–C)
	545m	550m						ν(Hg–C)
	340w	350m	340w					ν(Hg–S)

Table 7
^{13}C NMR spectroscopic data (ppm from $SiMe_4$)

Compound	C(2)[a]	C(4)	C(5)	C(6)	C(7)	C(8)	C(9)	MR^b_n
HL	180.25	110.43	125.07	123.71	109.91	148.17	131.21	–
HgMeL	168.18	117.13	124.01	123.23	109.37	151.51	142.15	8.90 (1483.6)
	167.54 [c]	118.51 [c]	124.37 [c]	–	109.93 [c]	149.79 [c]	142.47 [c]	10.790 (1439) [c]
HgPhL	168.02	117.22	124.04	123.29	109.44	151.63	142.23	157.17 (C_i), 137.06 (C_o) (111.9), 128.41 (C_m) (185.4), 128.05 (C_p) (18.6)
$TlMe_2L$ [d]	179.5	114.6	122.5	120.5	107.6	150.9	143.1	25.21 (2926.5)
$TlPh_2L$	178.51	114.92	123.12	121.26	108.24	151.02	142.69	(C_i) [e], 136.37 (C_o) (311.7), 128.66 (C_m) (459.8), 128.23 (C_p) (48.8)

[a] Numbering scheme:

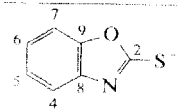

[b] Coupling constants, in Hz, in brackets. [c] Solid state. [d] Values from ref. 9. [e] Only the low field signal, at 206.95 ppm, was detected. The hight field one is overlapped.

a regular pentagon; (iii) The contribution of the SHgMe group is similar to that in methyl(pyrimidine-2-thiolato)mercury(II) [7].

The dipole moment calculated on the basis of this model, and with the methylmercury group placed in the ligand plane near the C=N group, is 2.3 D, which is satisfactorily close to the experimental value in view of the approximations involved. The calculated moment increases to 3.0 D if the HgMe group is placed in the ligand plane, but close to the oxygen atom of the oxazole ring. Assumption of free rotation of the organometallic group leads to a moment of 2.6 D [25]. Thus the experimental dipole moment seems to suggest for HgMeL a structure in benzene solution similar to that in the solid state. This conclusion probably applies also to HgPhL.

^{13}C NMR spectra

The main changes in the ^{13}C NMR spectrum when the ligand is S-methylated [26] or when its disulphur derivative is formed [27] (that is, when the thiol form is adopted), are mainly in the signals of the C(2), C(9), C(4) and C(8) atoms. C(2) is strongly shielded, probably due to formation of a N=C–S group in place of a N–C=S group [28]. On the other hand, the C(9), C(4) and C(8) atoms are deshielded. Similar behaviour is observed (Table 7) when the HgMeL compounds are formed, indicating a change in the ligand towards the thiol form. The position of the signals associated with the MeHg group also suggests the presence of a mercury–thiol bond [29].

In organothallium compounds the C(2) signal is close to that observed in the free ligand for this atom (see Table 7). This means that, in these compounds, there is little change in the ligand towards the thiol form. Correspondingly, the deshielding effects of TlR_2^+ coordination on the C(4) and C(8) signals are smaller than for the mercury derivatives. Nevertheless, the C(9) resonance appears at lower field in TlR_2L than in HgRL; the unexpected position of the signal from this carbon can be understood if the thallium atom interacts simultaneously with the ligand through the S and N atoms, as observed in compounds with similar characteristics [9,30]. The inductive effects of the Tl–N interaction must shift the C(9) signal downfield more than would be expected from the small thione-thiol movement in the ligand in TlR_2L.

The spectra of HgMeL in the solid state and in solution are closely similar other. In fact the changes observed (Table 7) are smaller than those found for the free ligand [31], perhaps because the mercury coordination fixed the thiol tautomeric form in both states. This spectra similarity again suggests that the structure of this compound does not change significantly upon dissolution in an organic solvent.

Acknowledgements

We thank the DGICYT (PB87-0482) for financial support, and J. Sanz and I. Sobrados and the Centro Nacional de RMN de Sólidos (Madrid) for the facilities for the ^{13}C CP/MAS measurements.

References

1 A.J. Carty, in F.E. Brinckman and J.M. Bellama (Eds.), Organometals and Organometalloids Occurrence and Fate in the Environment, ACS Symposium Series No. 82, American Chemical Society, Washington, D.C., 1978, p. 339.

2 L.G. Kuz'mina and Y.T. Struchkov, Croat. Chem. Acta, 57 (1980) 701.
3 A.T. Hutton, H.M.N.H. Irving, L.R. Nassimbeni and G. Gafner, Acta Crystallogr. Sect. B, 36 (1980) 2064.
4 J. Zukerman-Schpector, M.C. Rodriguez-Argüelles, M.I. Suárez, A. Sánchez, J.S. Casas and J. Sordo, J. Coord. Chem., in press.
5 J. Bravo, J.S. Casas, M.V. Castaño, M. Gayoso, Y.P. Mascarenhas, A. Sánchez, C.O.P. Santos and J. Sordo, Inorg. Chem., 24 (1985) 3435.
6 J. Bravo, J.S. Casas, Y.P. Mascarenhas, A. Sánchez, C.O.P. Santos and J. Sordo, J. Chem. Soc., Chem. Commun., (1986) 1101.
7 A. Castiñeiras, W. Hiller, J. Strähle, J. Bravo, J.S. Casas, M. Gayoso and J. Sordo, J. Chem. Soc., Dalton Trans., (1986) 1945.
8 H. Gilman and R.G. Jones, J. Am. Chem. Soc., 68 (1946) 517; J.J. Eisch, in J.J. Eisch and R.B. King (Eds.), Organometallic Syntheses, Vol. 2, Academic Press, New York, 1981, p. 154.
9 M.V. Castaño, A. Sánchez, J.S. Casas, J. Sordo, J.L. Briansó, J.F. Piniella, X. Solans, G. Germain, T. Debaerdemaeker and J. Glaser, Organometallics, 7 (1988) 1897.
10 N. Walker and D. Stuart, Acta Crystallogr., Sect. A, 39 (1983) 158.
11 G.M. Sheldrick, SHELX76, Program for Crystal Structure Determination, Univ. Cambridge, UK, 1976.
12 J.R. Masaguer, J.S. Casas, A. Sousa-Fernández and J. Sordo, An. Quim., 69 (1973) 199.
13 W.T. Dixon, J. Magn. Reson., 44 (1981) 220.
14 P. Groth, Acta Chem. Scand., 27 (1973) 945.
15 A.R. Norris, A. Palmer and A.L. Beauchamp, J. Cryst. Spectrosc. Res., 20 (1990) 23.
16 A.J. Canty and G.B. Deacon, Inorg. Chim. Acta, 45 (1980) L225.
17 M.S. García-Tasende, M.I. Suárez-Gimeno, A. Sánchez, J.S. Casas, J. Sordo and E.E. Castellano, J. Organomet. Chem., 384 (1990) 19.
18 J.A. Masucci and A.B. Reitz, Org. Mass Spectrom., 22 (1987) 233.
19 C. Preti and G. Tosi, Can. J. Chem., 55 (1977) 1409.
20 F.A. Devillanova and G. Verani, Aust. J. Chem., 33 (1980) 279.
21 S.L. Srivastava, M. Prasad, Rohitashava and R. Singh, Indian J. Phys., 61B (1987) 23.
22 (a) S. Jeannin, Y. Jeannin and G. Lavigne, Inorg. Chem., 17 (1978) 2103; (b) idem, ibid., 18 (1979) 3528.
23 W.J. Geary, Coord. Chem. Rev., 7 (1971) 81.
24 V.A. Granzhan, N. Poznanskaya, N.I. Shvetsov-Shilovskii, S.K. Laktionova and M.I. Kolesnik, Russ. J. Phys. Chem., 45 (1971) 1.
25 V.I. Minkin, O.A. Osipov and Tu.A. Zhdanov, Dipole Moments in Organic Chemistry, Plenum, New York, 1970, p. 100.
26 J. Llinares, J.P. Galy, R. Faure, E.J. Vincent and J. Elguero, Can. J. Chem., 57 (1979) 937.
27 E. Gründemann, D. Martin and A. Wenzel, Org. Magn. Reson., 12 (1979) 95.
28 A.M. Brodie, H.D. Holden, J. Lewis and J.M. Taylor, J. Chem. Soc., Dalton Trans., (1986) 633.
29 A.R. Norris, R. Kumar and E. Buncel, J. Inorg. Biochem., 22 (1984) 11, and ref. therein.
30 M.S. García-Tasende, M.I. Suárez, A. Sánchez, J.S. Casas, J. Sordo, E.E. Castellano and Y.P. Mascarenhas, Inorg. Chem., 26 (1987) 3818.
31 R. Faure, E.J. Vincent and J. Elguero, Heterocycles, 20 (1983) 1713.